# Comparing the loss of charge carrier generation with the loss of VOC at low temperatures in organic bulk-heterojunction blends

Wilson, N M; Aarnio, Harri; Österbacka, Ronald

*Published in:*
Physica Scripta

*DOI:*
10.1088/1402-4896/acff94

Published: 01/11/2023

*Document Version*
Accepted author manuscript

# Comparing the loss of charge carrier generation with the loss of $V_{OC}$ at low temperatures in organic bulk-heterojunction blends

**N M Wilson[1], H Aarnio[2] and R Österbacka[1]**

[1] Physics, Faculty of Science and Engineering, Åbo Akademi University, Henriksgatan 2, 20500 Turku, Finland
[2] Mathematics and physics, Centria University of Applied Sciences, Bondegatan 2, 67100 Karleby, Finland

E-mail: Ronald.Osterbacka@abo.fi

**Abstract.** We estimate the temperature dependence of charge carrier generation in P3HT:ICBA and PTB7:PCBM using continuous-wave photoinduced absorption. For P3HT:ICBA, the generation rate increases fivefold from 79 K to ca 250 K, above which it saturates. We compare this to the temperature dependence of open-circuit voltage ($V_{OC}$) which at low temperatures shows a decrease with decreasing temperatures, in disagreement with the typically expected linear rise. This voltage loss is too large to be explained by the decrease of generation with decreasing temperature. For PTB7:PCBM the dominant species has a generation rate increasing from 90 to 150 K, after which it decreases. For PTB7:PCBM there is no decrease in $V_{OC}$ at low temperatures. Our findings support the lack of correlation between the decrease in $V_{OC}$ and a decrease in generation rate. We conclude that the loss of $V_{OC}$ does not originate in charge carrier dynamics in the bulk material, but is due to contact effects.

*Keywords*: photoinduced absorption, continuous-wave photoinduced absorption, organic semiconductors, organic photovoltaics, organic solar cells, polymer:fullerene blends, charge carrier generation, open-circuit voltage
Submitted to: *Phys. Scr.*

## 1. Introduction

While organic solar cells are reaching higher efficiencies year by year, there is still much discussion about the physics underlying charge carrier generation. Here we study two low-mobility polymer:fullerene blends with an efficient dissociation of electrons and holes at the donor-acceptor interface. In addition to a high generation rate, an efficient solar cell requires low recombination and efficient extraction. All these factors affect the open-circuit voltage ($V_{OC}$), which is often used to characterize solar cells. The commonly used theories for describing $V_{OC}$ predict a temperature dependence in which $V_{OC}(T)$ increases linearly, or possibly saturates, when lowering the temperature of the sample [1]. As previously observed in some polymer:fullerene blends we measure

a decreasing $V_{OC}$ with lower temperatures [2, 3]. Gao et al. suggested that this is due to the decreased influence of entropy on the free energy at lower temperatures causing poorer charge separation [2]. Other effects at the bulk-heterojunction interface could also be crucial for the temperature dependence of charge generation, such as delocalization [4]. To cause a $V_{OC}$ that decreases with temperatures a drastic decrease in generation rate is needed. This can be seen in the logarithmic nature of the generation rate dependence of $V_{OC}$ competing with the linear temperature dependence, here given for recombination with the reaction order $\delta$ [5]:

$$eV_{OC} = E_g - \frac{2}{\delta}kT \ln\left(\frac{b(N_C N_V)^{\delta/2}}{G}\right). \quad (1)$$

Here $e$ is the elementary charge, $E_g$ is the bandgap, $k$ is the Boltzmann constant, $N_{C(V)}$ is the density of states in the conduction (valence) band and $G$ is the generation rate for carriers. The recombination constant $b$ and reaction order $\delta$ are introduced to approximately describe the dynamics of the charge carrier density $n$ through

$$\frac{dn}{dt} = G - bn^{\delta}. \quad (2)$$

Setting $\delta = 2$ gives the corresponding equations for bimolecular recombination. Note that (1) holds for constant photogeneration throughout the solar cell and assumes perfectly selective contacts.

At $V_{OC}$ the system is at steady-state where all generated charges will recombine and $dn/dt = 0$. This means that the value of $V_{OC}(T)$ will, in the ideal case, be determined solely by the generation and recombination in the bulk. However, $V_{OC}(T)$ can also be limited by contact properties, such as extraction and surface recombination [6]. In this paper, we estimate how $V_{OC}(T)$ would behave for a device with perfect contacts by using continuous-wave photoinduced absorption (cwPA). This is an optical pump-probe technique that does not rely on contacts. As there is no extraction, all generated carriers will recombine within the sample. By measuring the optical signal of the charge carriers we obtain information about generation and recombination dynamics for long-lived charge carriers [7, 8, 9, 10, 11]. We measured the generation in two different blends and compared samples made with different contacs, and found that bulk effects are not the reason for the loss of $V_{OC}$ at low temperatures.

## 2. Methods

### *2.1. Open-circuit voltage*

We have measured current versus voltage (IV-curves) under illumination for three devices with poly(3-hexylthiophene) (P3HT) and indene-C60 bisadduct (ICBA) in a 1:1 blend as an active layer. Samples 1 and 2 had the structure ITO/PEDOT:PSS/ P3HT:ICBA/LiF/Al and were manufactured from the same solution, but sample 2 was left in the glove box for 8 days before measuring, causing degradation in the form of extraction barriers. Sample 3 had the same structure but with $MoO_3$ instead of PEDOT:PSS. The use of $MoO_3$ is known to cause doping [12]. For a fourth sample we used PTB7:PCBM in the structure ITO/PEDOT:PSS/PTB7:PC70BM/LiF/ Al with PTB7:PCBM in a 1:1.5 ratio. The samples were mounted in a cryostat and

$V_{OC}(T)$ was extracted from the IV-curves at different temperatures. We used an argon ion laser for photogeneration (at 514 nm) at an intensity corresponding to 1 sun (for PTB7:PCBM and P3HT:ICBA samples 1 and 2). The intensity was adjusted so the room temperature IV-curves matched those measured under a solar simulator as closely as possible. For P3HT:ICBA sample 3 the intensity was approximately two times as high. For details on sample preparation and experimental setup see the supplementary material.

### *2.2. Continuous-wave photoinduced absorption*

To disentangle the effects of generation and recombination from the influence of contacts we have used continuous-wave photoinduced absorption (cwPA). This optical measurement is performed on a thin film. The physical conditions are similar to those of the ideal $V_{OC}$ measurement, as all carriers that are generated will also recombine. The cwPA-setup is discussed in more detail in the supplemental material and the preceding article [13].

For cwPA the samples were prepared by spin-coating the active material on sapphire substrates. The P3HT:ICBA sample was prepared in a 1:1 weight ratio. The PTB7:PCBM sample was prepared in a 1:1.5 weight ratio with the addition of 1,8-diiodooctane (DIO). As our conclusions are of a general nature and do not concern exact values we maintain that a comparison of this sample with the one manufactured for $V_{OC}$ is valid despite the lack of DIO in the sample used for $V_{OC}$.

The cwPA measurement is a pump-probe technique where charge carriers are generated with a laser that is modulated so that its intensity varies periodically. For the results presented here, we used an argon ion laser emitting at 514 nm and a sinusoidal modulation (unless otherwise stated). The probe light was a continuous spectrum lamp, the absorption of which depends on the number of charge carriers in the sample. To acquire reliable results from cwPA it is crucial to recognize limitations of the setup and correct them, as discussed in the preceding article [13].

In a cwPA measurement with a sinusoidal pump light the system is at a quasi-steady state with a generation rate that varies as $\frac{G}{2}(\sin\omega t + 1)$. The change in transmission caused by the pump light is assumed to be directly proportional to $n\sigma d$, i.e. the change in charge carrier density $n$, the absorption cross section $\sigma$ and the film thickness $d$. By choosing a probe wavelength corresponding to the absorption of a specific excitation species, we monitor the density of that species, and thereby gain information about generation and recombination dynamics.

A periodic pump light is used in order to eliminate all noise at other frequencies than $\omega$, but as a consequence the results are obtained in the frequency domain. The signal is recorded by a lock-in amplifier as in-phase ($PA_{\mathrm{I}}$) and quadrature ($PA_{\mathrm{Q}}$), which have the same frequency as the pump light and a phase shift of 0 and $\pi/2$, respectively. As we discuss in the preceding article, for P3HT:ICBA we study the radius signal $PA_{\mathrm{R}} = \sqrt{PA_{\mathrm{I}}^2 + PA_{\mathrm{Q}}^2}$, to avoid errors resulting from unknown phase shifts in the detector [13]. For PTB7:PCBM we use another detector, that allows for the analysis of the more detailed information found in $PA_{\mathrm{I}}$ and $PA_{\mathrm{Q}}$. An analytical

approximation, based on bimolecular recombination, for cwPA with sinusoidal pump light was given by Westerling et al [14].

$$PA_{\mathrm{I}}(G,\omega) = \frac{G\tau}{2}\left(\frac{\sqrt{F(\omega,\tau)}}{(\omega\tau)^2 + F(\omega,\tau)}\right)\sigma d \tag{3}$$

$$PA_{\mathrm{Q}}(G,\omega) = \frac{G\tau}{2}\left(\frac{\omega\tau}{(\omega\tau)^2 + F(\omega,\tau)}\right)\sigma d \tag{4}$$

where

$$F(\omega,\tau) = 1 - \frac{(\omega\tau)^2}{2} + \frac{1}{2}\sqrt{\left((\omega\tau)^2+2\right)^2 - 2}$$

Several studies have demonstrated that this equation does not always adequately fit measured data. This is attributed to the presence of dispersion, originating in relaxation processes. In cwPA this is often included by using a Cole-Cole type function. [15, 16, 17, 18] The results are given by

$$PA_{\mathrm{I}} = \frac{G\tau\sigma d[1+\cos(\frac{\pi\alpha}{2})(\omega\tau)^{\alpha}]}{1+2(\omega\tau)^{\alpha}\cos(\frac{\alpha\pi}{2})+(\omega\tau)^{2\alpha}} \tag{5}$$

$$PA_{\mathrm{Q}} = \frac{G\tau\sigma d\sin(\frac{\pi\alpha}{2})(\omega\tau)^{\alpha}}{1+2(\omega\tau)^{\alpha}\cos(\frac{\alpha\pi}{2})+(\omega\tau)^{2\alpha}} \tag{6}$$

$$PA_{\mathrm{R}} = \frac{G\tau\sigma d}{\sqrt{1+2(\omega\tau)^{\alpha}\cos(\frac{\alpha\pi}{2})+(\omega\tau)^{2\alpha}}}, \tag{7}$$

where the dispersion constant $0 < \alpha < 1$ accounts for more dispersive behavior the further it is from 1.

## 3. Results

### *3.1. Temperature-dependent $V_{OC}$*

The open-circuit voltage as a function of temperature is shown in figure 1. All curves follow a linear dependence on temperature at high temperatures. This is in accordance with the formalism used to describe $V_{OC}$, represented in (1). The plot for PTB7:PCBM is linear down to low temperatures and has a similar shape to that measured by Ebenhoch et al. for PTB7:PCBM with DIO added [19]. For P3HT:ICBA there is, however, a clear deviation from the linear behavior at low temperatures. Equation (1) indicates that a steep decrease in $G$ or a change in recombination dynamics could be the cause. In addition, $V_{OC}$ can be influenced by limitations at the contacts [20, 6].

### *3.2. Temperature-dependent cwPA*

The photoinduced absorption spectrum for a film of P3HT:ICBA is seen in the inset in figure 2a at 79 K with an excitation at 514 nm. To measure the spectrum we used a square wave pump light modulated by a mechanical chopper. The result is a spectrum with a peak at 1.26 eV corresponding to a localized polaron (P2) and a broader signature above 1.6 eV corresponding to a delocalized polaron (DP2) [21, 22]. All subsequent measurements were made at 1.26 eV (985 nm). The spectrum for PTB7:PCBM, seen in the inset in figure 2b, has a similar form with a peak at 1.10 eV

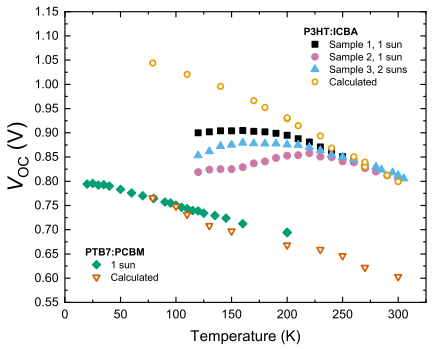


**Figure 1.** Open-circuit voltage as function of temperature. Full symbols show results measured on three P3HT:ICBA and one PTB7:PCBM solar cell. Open symbols show $V_{OC}(T)$ calculated from cwPA via (8).

overlapping with a broader band. These have been attributed to polarons (P2) and triplet excitons [23, 24]. For this blend, we study cwPA slightly above the peak, at 1.18 eV (1050 nm).

The radius signal as a function of frequency for P3HT:ICBA is shown in figure 2a. In the regime where $\omega\tau \gg 1$, equation (7) approaches $G\sigma d\tau^{1-\alpha}\omega^{-\alpha}$, and thus we expect the signal to be almost independent of lifetime and be directly proportional to the generation rate. For a non-dispersive response, there would be no dependence on $\tau$, while dispersion leaves a weak dependence $\tau^{1-\alpha}$. In light of this, we can see from the data in figure 2a that the effective generation rate increases with increasing temperature and becomes constant at high temperatures. To extract $G(T)$ and $\tau(T)$, we fitted the curves with (7) ($\sigma = 10^{-16}$ cm$^2$, $d = 300$ nm).

The parameters acquired from the fit of the PA data are presented in figure 4a, showing an effective generation rate that increases as the temperature rises, until $T \approx 250$ K, at which $G$ saturates. The increase is significant, approximately fivefold. The saturation suggest that some step in the generation process is controlled by an energy threshold of around 22 meV. The results and procedure are similar to those by Koerner et al. in quaterthiophene:C60 films [10]. The plot of $\tau(T)$ is consistent with the general shape expected for trap-assisted recombination with a trap depth close to $kT$ at room temperature, as the lifetime starts to increase significantly when going below ca 250 K. Other cwPA work has shown that the dominant recombination mechanism in this blend is trap assisted in an exponential distribution with a trap depth of $E_{ch} \approx 24$ meV (equivalent to kT at 279 K) [22]. The fits of the PA data in figure 2 also give a weak temperature dependence of the dispersion constant $\alpha$, shown in the supplementary material.

The radius signal as a function of frequency for PTB7:PCBM is plotted in figure 2b. Here, the curves never reach the linear slope predicted for $\omega\tau \gg 1$, impeding immediate conclusions about $G(T)$. By studying this sample with a different detector we can access the in-phase and quadrature in figure 3, as explained in the preceding

article [13]. For clarity, only a selection of the temperature-dependent curves is plotted, while the rest can be found in the supplementary material. Fitting $PA_I$ and $PA_Q$ instead of just $PA_R$ means we access more information about the dynamics. The quadrature in figure 3b has a broad knee connecting the low- and high-frequency regimes, calling for a two component fit. To avoid overfitting when using two lifetimes and two generation rates we assume negligible dispersion and switch to equations (3)-(4). The resulting temperature-dependent parameters are presented in figure 4b. Species 1 (described by $G_1$ and $\tau_1$) has a generation rate with a peak at 150 K and is a significantly larger than species 2 (described by $G_2$ and $\tau_2$). Species 2 has a generation rate that increases with decreasing temperatures, and both the generation rate and lifetime are so low at high temperatures (above ca 200 K) that it would not be necessary to include this species in order to achieve a good fit. For both species the lifetimes increase with decreasing temperature. Using just one excitation species and fitting the data with (5)-(6) gives a slightly poorer fit, shown in the supplemental material alongside resulting parameters. The parameters' behaviour is similar to that of $G_1$ and $\tau_1$.

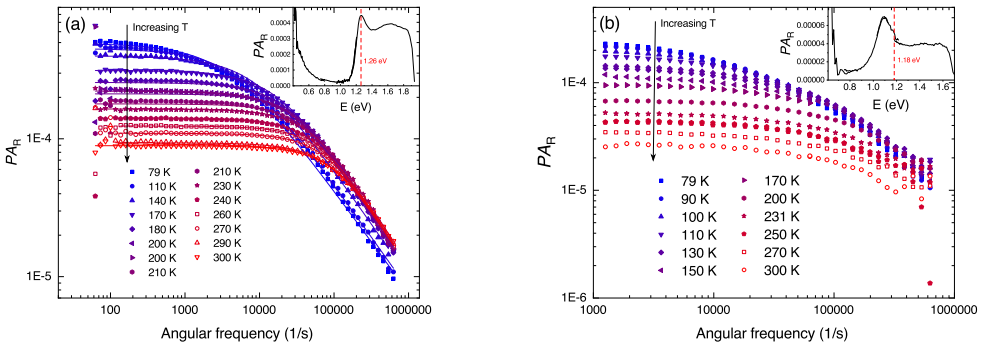


**Figure 2.** $PA_R$ as a function of frequency for different temperatures for (a) P3HT:ICBA and (b) PTB7:PCBM. The insets show the photoinduced absorption spectra, with the energy used in the frequency dependence marked with a dashed line.

## 4. Discussion

As we have extracted information about generation and recombination, we can now recreate $V_{OC}(T)$ for a device in the ideal case, not limited by contacts. To rewrite (1) using the lifetime obtained from cwPA we assume that the recombination in (2) can be rewritten as monomolecular recombination with an effective lifetime $\tau$, i.e. $bN^\delta = N/\tau$. This is the same type of definition as that of a bimolecular lifetime used in (3)-(4) [14]. We also assume that we are close to steady state, therefore $\mathrm{d}N/\mathrm{d}t = 0$ and $N = (G/b)^{1/\delta}$. This leads to $G/b = \tau^\delta G^\delta$ which inserted into (1) gives

$$qV_{oc} = E_g - 2kT \ln\left(\frac{(N_C N_V)^{1/2}}{G\tau}\right) \tag{8}$$

For both PTB7:PCBM and P3HT:ICBA we insert $\tau(T)$ and $G(T)$ from fits with one

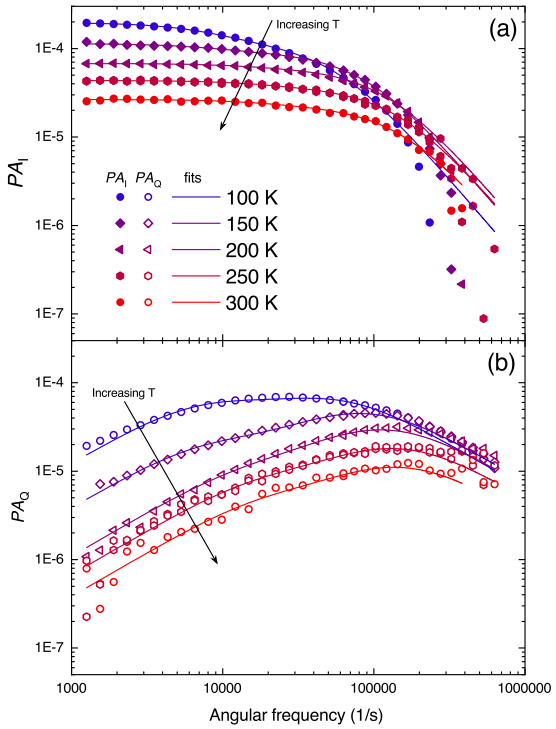


**Figure 3.** $PA_I$ and $PA_Q$ for PTB7:PCBM. For clarity, only a selection of the curves is shown, the rest are shown in the supplementary material. Fits with (3)-(4) with two sets of parameters.

dominant species. The results are plotted in figure 1 alongside $V_{OC}$-data from measurements on real devices. For the other parameters in 8 we used $E_g = 1.1$ eV and $N_C = N_V = 10^{19}$ cm$^{-3}$ for P3HT:ICBA and $E_g = 0.8$ eV and $N_C = N_V = 10^{18}$ cm$^{-3}$ for PTB7:ICBA. The value for $E_g$ was chosen by extrapolating the high temperature $V_{OC}(T)$ slopes, and the band densities to fit the values for the high temperature $V_{OC}(T)$. Neither of the $V_{OC}(T)$-plots calculated from $G(T)$ and $\tau(T)$ show a decrease with lower temperatures, but a tendency towards saturation can be seen for P3HT:ICBA. We thus conclude that effects in the bulk heterojunction material are not responsible for the decrease in $V_{OC}$ at low temperatures.

On the other hand, it is highly plausible that contacts are the reason for the observed $V_{OC}(T)$. To explore this possibility, we study the JV-curves (current density-voltage-curves) of the three P3HT:ICBA devices, shown in figure 5 (curves for lower temperatures are presented in the supplemental information). Sample 1, which was measured directly after manufacturing displays a markedly different shape than sample 2 which was left in the glove box for 8 days before measuring. Sample 2 displays a clear S-shaped JV-curve, indicating poor majority carrier extraction at the contacts [25]. Sample 3 is known to be weakly doped due to the use of $MoO_3$, which could cause the reduced photocurrent [26]. Sample 1, which suffers the least from doping and

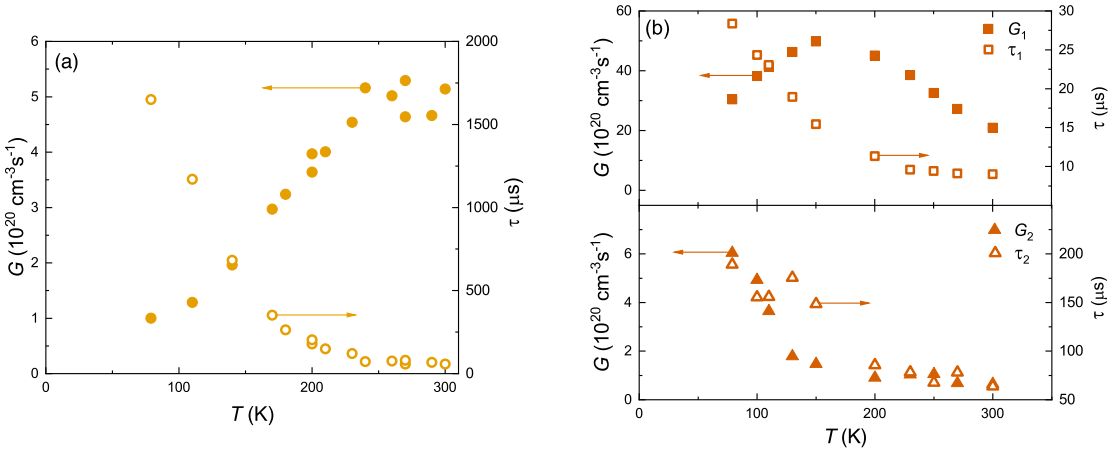


**Figure 4.** Parameters extracted from fits for (a) P3HT:ICBA and (b) PTB7:PCBM. In (a) equation (7) was used to fit plots in figure 2, resulting in temperature-dependent $G$ and $\tau$. In (b) two sets of equations (3)-(4) with different parameters (one with $G_1$ and $\tau_1$, the other with $G_2$ and $\tau_2$) were added and produced the fits in figure 3.

contact limitations, also reaches the highest $V_{OC}(T)$ in figure 1. These observations confirm that the $V_{OC}(T)$ decrease is linked to extrinsic effects such as poor contacts or unintentional doping.

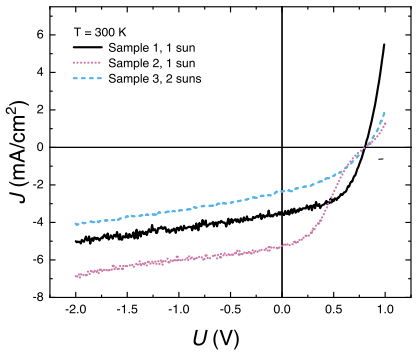


**Figure 5.** Example of JV-curves for the three P3HT:ICBA devices at 300 K.

## 5. Conclusions

We used cwPA to determine the temperature dependence of the charge carrier generation rate in two low-mobility polymer:fullerene solar cell materials. As a contact-less technique, cwPA allows investigation of recombination and generation in the bulk of materials used for photovoltaic applications. From the acquired generation rate and

lifetime we have calculated $V_{OC}(T)$ for a solar cell without contact limitations, and compare it to experimentally measured $V_{OC}(T)$. The calculated $V_{OC}$ fails to reproduce the loss of $V_{OC}$ seen at low temperatures for one of the studied blends. These results affirm that intrinsic effects in the bulk-heterojunction blend do not cause the temperature-dependent loss of $V_{OC}$ at low temperatures, which we suggest are due to contact related effects.

## References


[1] Würfel P 2005 *Physics of Solar Cells* (Weinheim: Wiley-VCH) ISBN 3-527-40428-7

[2] Gao F, Tress W, Wang J and Inganäs O 2015 *Physical Review Letters* **114** 1–5 ISSN 10797114 URL https://doi.org/10.1103/PhysRevLett.114.128701

[3] Thakur A K, Wantz G, Garcia-Belmonte G, Bisquert J and Hirsch L 2011 *Solar Energy Materials and Solar Cells* **95** 2131–2135 ISSN 09270248 URL https://doi.org/10.1016/j.solmat.2011.03.012

[4] Tscheuschner S, Bässler H, Huber K and Köhler A 2015 *Journal of Physical Chemistry B* **119** 10359–10371 ISSN 15205207 URL https://doi.org/10.1021/acs.jpcb.5b05138

[5] Nyman M, Sandberg O J and Österbacka R 2014 *Advanced Energy Materials* **5** URL https://doi.org/10.1002/aenm.201400890

[6] Sandberg O J, Sundqvist A, Nyman M and Österbacka R 2016 *Physical Review Applied* **5** 044005 ISSN 2331-7019 URL http://link.aps.org/doi/10.1103/PhysRevApplied.5.044005

[7] Botta C, Luzzati S, Tubino R, Bradley D and Friend R H 1993 *Physical Review B* **48** URL https://doi.org/10.1103/PhysRevB.48.14809

[8] Wohlgenannt M, Graupner W, Leising G and Vardeny Z V 1999 *Physical Review B* **60** 5321–5330 URL https://doi.org/10.1103/PhysRevB.60.5321

[9] Westerling M, Österbacka R and Stubb H 2002 *Physical Review B* **66** 1–7 URL https://doi.org/10.1103/PhysRevB.66.165220

[10] Koerner C, Ziehlke H, Gresser R, Fitzner R, Reinold E, Bäuerle P, Leo K and Riede M 2012 *Journal of Physical Chemistry C* **116** 25097–25105 ISSN 19327447 URL https://doi.org/10.1021/jp307582a

[11] Lafalce E, Jiang X and Zhang C 2011 *Journal of Physical Chemistry B* **115** 13139–13148 ISSN 15205207 URL https://doi.org/10.1021/jp2066666

[12] Nyman M, Dahlström S, Sandberg O J and Österbacka R 2016 *Advanced Energy Materials* **6** 6–11 ISSN 16146840 URL https://doi.org/10.1002/aenm.201600670

[13] Wilson N M, Aarnio H and Österbacka R Submitted concurrently with this article

[14] Westerling M, Vijila C, Österbacka R and Stubb H 2003 *Chemical Physics* **286** 315–320 ISSN 03010104 URL https://doi.org/10.1016/S0301-0104(02)00930-8

[15] Epshtein O, Nakhmanovich G, Eichen Y and Ehrenfreund E 2001 *Physical Review B* **63** 2–7 ISSN 0163-1829 URL https://doi.org/10.1103/PhysRevB.63.125206

[16] Cole K S and Cole R H 1941 *J. Chem. Phys.* **9** 98–105 ISSN 00219606 URL https://doi.org/10.1063/1.1750906

[17] Metzler R and Klafter J 2002 *Journal of Non-Crystalline Solids* **305** 81–87 URL https://doi.org/10.1016/S0022-3093(02)01124-9

[18] Westerling M, Vijila C, Österbacka R and Stubb H 2004 *Physical Review B* **69** 1–8 ISSN 01631829 URL https://doi.org/10.1103/PhysRevB.69.245201

[19] Ebenhoch B, Thomson S A, Genevičius K, Juška G and Samuel I D 2015 *Organic Electronics* **22** 62–68 ISSN 1566-1199 URL https://doi.org/10.1016/j.orgel.2015.03.013

[20] Rauh D, Wagenpfahl A, Deibel C and Dyakonov V 2011 *Applied Physics Letters* **98** ISSN 00036951 (*Preprint* 1110.0588) URL https://doi.org/10.1063/1.3566979

[21] Singh S, Pandit B, Hukic-markosian G, Basel T P and Vardeny Z V 2012 *Journal of Applied Physics* **123505** URL http://dx.doi.org/10.1063/1.4769211

[22] Sandén S, Wilson N M, Nyman M and Österbacka R 2017 *Organic Electronics* **42** 131–140 ISSN 15661199 URL http://dx.doi.org/10.1016/j.orgel.2016.12.017

[23] Basel T, Huynh U, Zheng T, Xu T, Yu L and Vardeny Z V 2015 *Advanced Functional Materials* URL https://doi.org/10.1002/adfm.201403191

[24] Baniya S, Vardeny S R, Lafalce E, Peygambarian N and Vardeny Z V 2017 *Physical Review Applied* **7** 1–9 ISSN 23317019 URL https://doi.org/10.1103/PhysRevApplied.7.064031

[25] Wagenpfahl A, Rauh D, Binder M, Deibel C and Dyakonov V 2010 *Physical Review B* **82**(11) 115306 ISSN 1098-0121 URL https://doi.org/10.1103/PhysRevB.82.115306

[26] Sandberg O J, Dahlström S, Nyman M, Wilken S, Scheunemann D and Österbacka R 2019 *Physical Review Applied* **12** 1 ISSN 2331-7019 URL https://doi.org/10.1103/PhysRevApplied.12.034008

## Acknowledgments

Frans Jansson is acknowledged for fabricating and performing measurements on P3HT:ICBA sample 3. Partial financial support from the Academy of Finland through the project No. 279055 is acknowledged. Personal grants from Otto A. Malm foundation, Alfred Kordelin Foundation, Fortum and Neste Foundation and The Swedish Cultural Foundation in Finland are acknowledged by N.M.W.